Desalination and Water Treatment
www.deswater.com
doi: 10.5004/dwt.2019.23860

149 (2019) 117–128
May

Treatment of aluminum hot-rolled waste emulsion by coagulation–flocculation

Qing Zhong[a,b], Yingyue Zhu[a,b], Zhanqiang Wang[a,b], Bo Liu[a,b], Xizhi Zouhu[a,b], Yuqin Tian[c], Rongjiao Zhu[a,b,*]

[a]*Department of Chemistry, School of Science, Tianjin University, Tianjin 300072, China, Tel. +86 13821621113; Fax: +86-22-27403475; email: zhurongjiao@tju.edu.cn (R. Zhu), Tel. +86 18302223964; email: 2698219171@qq.com (Q. Zhong), Tel. +86 15522007261; email: 2211899285@qq.com (Y. Zhu), Tel. +86 18526644027; email: wangzhanqiang2013@126.com (Z. Wang), Tel.+86 15822637366; email: 2403210959@qq.com (B. Liu), Tel.+86 15620504054; email: soni19931118@163.com (X. Zouhu)*
[b]*Collaborative Innovation Center of Chemical Science and Engineering (Tianjin), Tianjin 300072, China*
[c]*Petroleum engineering technology research institute, Shengli oil field branch, SINOPEC, Dongying 257000, China, Tel.+86 15022736261; email: 457380246@qq.com*

Received 13 July 2018; Accepted 24 January 2019

ABSTRACT

Aluminum hot-rolled waste emulsion (AWE) which possessed the properties of high oil content, chemical oxygen demand (COD) and organic pollutants became difficult to treat and demulsify in a traditional way. In the light of the common inorganic demulsifier poly aluminum silicate chloride (PASC), a novel demulsifier epichlorohydrin amine cationic polymer (FP-1) made by our laboratory was added to achieve the effect of complete demulsification. The treatment of AWE was optimized by dint of employing the response surface method and Box–Behnken design to determine the optimal conditions of PASC dose, FP-1 dose and pH. The experimental results which were consistent with the polynomial model predictions demonstrated that oil and COD removal efficiencies of 97.1% and 91.5%, could be achieved by dint of utilizing 1.45 g L^{-1} PASC, 2.22 g L^{-1} FP-1 and pH 5.14 at 328 K for 50 min. The demulsification process was studied by morphology analysis, infrared spectrum analysis and zeta potential analysis.

Keywords: Aluminum hot-rolled waste emulsion (AWE); Response surface method (RSM); Coagulation–flocculation; Oil removal; COD removal

1. Introduction

Aluminum and aluminum alloys widely employed in the metal manufacturing and transportation industry are produced by the hot-rolling process [1,2]. In this process, the recycle lubricant which contains base oil and varieties of additives were added to prevent the adhesion of aluminum and water was used as the coolant [3–7]. Then numerous oil/water (O/W) waste emulsion were formed which would deteriorate after employing a long time. It is a difficult process for aluminum plants as the large amount of aluminum hot-rolled waste emulsion (AWE) containing varieties of organic pollutants, oil, metal cation and surfactants is difficult to store and handle. Consequently, the treatment of AWE has become an urgent concern.

It is known that varieties of methods were employed to deal with AWE containing acidification and electrolysis. Johnsson et al. [8] investigated that the recovered emulsion of aluminum alloy 3005 treated with the polymer-based flocculant generated lower rolling force than with azelaic acid and indicated that the polymer-based flocculation produced a somewhat larger droplet size causing better plate-out and thicker oil film than acidification. Han [9] designed an electrolytic demulsification device of AWE. Notwithstanding the fact that the vast majority of energy was consumed and

* Corresponding author.

more Cl_2 and H_2 were released by electrolysis. Generally with the growth of electrolysis time, the electrode was thickened in view of the adhesion of the oil layer and replaced frequently.

Existing studies have demonstrated that the combination of inorganic and organic flocculants can play their own advantages and reach the acceptable flocculation effect [10–17]. For organic cationic flocculants, epichlorohydrin amine cationic polymer (FP-1) which was an effective water-soluble coagulant with organic cations containing nonpolar groups, could develop a net positive charge and become sufficiently hydrophobic for anionic and non-ionic organic contaminants removal from wastewater [18–21].

The experimental design of flocculation was lenient to be operated by one-factor at-a-time approach which had the limitations of time-consuming and the ignoring of interactions among variables [22–25]. Researchers have found that the flocculation efficiency influenced by varieties of factors [26–33] can be optimized by the response surface method legitimately [24,34–38]. Response surface methodology (RSM) was a scientific statistical method being employed to design experimental models, investigate the interactions of complex factors and determine the optimum theoretical conditions [23,24,39]. In the case of the same numbers of factors, the Box–Behnken design (BBD) which was utilized to evaluate nonlinear factors became more economical than central composite design in RSM [40].

In the literature, the demulsification of O/W emulsions has attracted increasing attention [41–47]. Few reports have been systemically researched on the coagulation–flocculation method and behavior of AWE with inorganic and organic flocculants until now. In addition, extremely high oil content and stability, the most critical problems have not drawn sufficient research attention. In our previous studies, poly aluminum silicate chloride (PASC) cannot demulsify AWE by coagulation–flocculation. The objective of the current research is to determine the optimum condition of treating AWE which was from Henan in China and had been stored in storage tanks for almost 6 months by dint of employing the composite flocculants of FP-1 and PASC via RSM. At the same time, the mechanism of coagulation–flocculation process was explored by morphology analysis, infrared spectrum analysis, and zeta potential analysis. The effective treatment method that had been developed in this study may provide a theoretical basis for the treatment of O/W emulsion with high oil content and stability.

2. Materials and methods

2.1. Materials

AWE was collected from aluminum factory in Henan province. Physicochemical analyses of the sample are shown in Table 1. FP-1 was developed by dimethylamine, epichlorohydrin, and butylamine by cross-linking polymerization.

2.2. Demulsification test

Coagulation–flocculation experiments were performed in 500 mL volume beakers with 400 mL of AWE and a magnetic stirrer. The pH of the AWE was adjusted to the varied levels by the addition of appropriate amounts of acid [37]. AWE was heated to 55°C and stirred (600 rpm) for 5 min.

Table 1
Characteristics of samples

Characteristics	Value
Color	Milky
Density (303 K) (g cm^{-3})	1.002
Viscosity (303 K) (mPa s)	0.9462
pH	5.166
Zeta potential (mV)	–37.4
Oil content (mg L^{-1})	39,008
COD content (mg L^{-1})	56,700

Certain amounts of PASC were then added to the waste emulsion with 1,200 rpm stirring for 3 min simultaneously. Finally, FP-1 was added to the waste emulsion with rapid stirring at 1,200 rpm for 3 min. Once all flocculants were added, the solution was slowly stirred at 600 rpm for 7 min and placed in the water baths at desired temperatures and different periods of settling time. The oil content and COD of aqueous phase at 8 cm below the oil surface was measured and at the same time removal efficiencies were calculated with Eqs. (1) and (2):

$$R = \frac{\left(C_0 - C_d\right)}{C_0} \times 100\% \tag{1}$$

where R is the oil removal efficiency, C_0 is the original oil content in the AWE (mg L^{-1}), and C_d is the oil content in the treated aqueous phase (mg L^{-1}).

$$R' = \frac{\left(D_0 - D_d\right)}{D_0} \times 100\% \tag{2}$$

where R' is the COD removal efficiency, D_0 is the original COD content in the AWE (mg L^{-1}), and D_d is the COD content in the treated aqueous phase (mg L^{-1}).

2.3. Experimental design and data analysis

Design-Expert software was employed to perform the experimental design, data analysis, and optimization design [30]. The three variables covering PASC dose (1.2, 1.5, and 1.8 g L^{-1}), FP-1 dose (2.0, 2.2, and 2.4 g L^{-1}), and pH (4, 5, and 6) that are listed in Table 2 have been investigated as key parameters which affected the two response parameters (oil removal and COD) in coagulation–flocculation process. The dosages were determined by the single-factor tests in the previous studies. The experimental design factors and level coding values are manifested in Table 2.

A response model for predicting the optimal conditions, and describing the relationship between the response value and factors, can be expressed in line with Eq. (3) [37,48].

$$Y_m = b_0 + \sum_{i=1}^{k} b_i X_i + \sum_{i=1}^{k} b_{ii} X_i^2 + \sum_{i}^{i<j} \sum_{j} b_{ij} X_i X_j \tag{3}$$

where Y_m is the predicted response value; b_0, b_i, b_{ii}, and b_{ij} are the offset term, ith linear coefficient, iith quadratic coefficient,

Table 2
Box–Behnken experimental design factors and level coding values

Factor	Name	Low actual (–1)	High actual (1)	Central actual (0)
X_1	PASC, g L^{-1}	1.2	1.8	1.5
X_2	FP-1, g L^{-1}	2.0	2.2	2.4
X_3	pH	4	5	6

and *ij*th interaction coefficient, respectively [30]. And X_i and X_j are the independent factors in coded units [49]. The observed results of the experimental design are listed in Table 3.

2.4. Optical microscope

Sudan dye is a fat-soluble dye. As fat-containing specimens encounter Sudan dyes, Sudan dye is dissolved in the fat-containing structure, which demonstrates color. Droplet microstructure changes of AWE before and after flocculation were observed by dint of utilizing optical microscope.

2.5. Fourier transform infrared spectroscopy (FTIR) spectra analysis

The structure of FP-1 was analyzed on an ALPHA FTIR Bruker (Beijing) Technology Co., Ltd., in the range 4,000–400 cm^{-1}. Sample of the oil from AWE and the oil from AWE with added FP-1 was dispersed (KBr) on a ALPHA FTIR (Bruker, Beijing) to determine the modification.

2.6. Zeta potential

The significance of zeta potential lies in its value related to the stability of the colloidal dispersion. To obtain further insight into their coagulation–flocculation process, the zeta potentials of AWE before and after the flocculation were measured on Zetasizer nano ZS90 at 298 K.

2.7. Scanning electron microscope and energy dispersive spectrometer

A sample of the flocs from the treated AWE was prepared for scanning electron microscope (SEM) and energy dispersive spectrometer (EDS) analysis by ethanol washing. SEM and EDS of the treated samples were performed utilizing Tecnai G2 F20 equipped with an EDS.

3. Results and discussion

3.1. Analysis of oil removal

The measured oil removal efficiencies listed in Table 3 is a significant indication for the coagulation–flocculation treatment efficiency [35]. The regression model with the experimental data for oil removal was presented by the following equation:

$$Y_1 = 95.68 - 2.60X_1 + 1.23X_2 + 2.45X_3 - 0.27X_1X_2 - 0.075X_1X_3 + 0.27X_2X_3 - 8.50X_1^2 - 8.40X_2^2 - 9.20X_3^2 \quad (4)$$

Table 3
BBD and response results for the study of three experimental variables

Run	Factor				Response
	PASC (X_1)	FP-1 (X_2)	pH (X_3)	Oil removal rate (%)	COD removal rate (%)
1	−1	−1	0	80.5	75.4
2	1	−1	0	74.7	69.6
3	−1	1	0	83.4	78.8
4	1	1	0	76.5	71.1
5	−1	0	−1	77.4	72.7
6	1	0	−1	73.5	67.9
7	−1	0	1	82.6	77.2
8	1	0	1	78.4	73.8
9	0	−1	−1	74.7	69.2
10	0	1	−1	76.7	70.9
11	0	−1	1	78.9	73.4
12	0	1	1	82.0	77.5
13	0	0	0	96.1	90.3
14	0	0	0	95.2	89.7
15	0	0	0	95.3	89
16	0	0	0	95.5	89.3
17	0	0	0	96.3	90.1

Analysis of variance (ANOVA) indicating the evaluation of the fitting response surface model was demonstrated in Table 4 [50]. The *F*-value of the model (250.68) with a *p*-value less than 0.0001 implied that the model was significant [51]. The justifiability of the model for reflecting the influences between the parameters can be manifested by the coefficient of determination (R^2 = 0.9969) correctly [52]. The accuracy of response prediction of the model can be evaluated by the predicted R^2: if the predicted and adjusted R^2 values are within approximately 0.20 then it is reasonable for the model or the data [35]. In the case of oil removal, the predicted R^2 value (0.9623) is in reasonable agreement with the adjusted R^2 value (0.9929). The *p*-values for lack of fit (0.1179) demonstrated that the *F*-value was insignificant, implying there is 11.79% chance that a "lack of fit *F*-value (3.73) " could occur due to noise. A signal to noise ratio of 4 or more (adequate precision) was a measure of the predicted response relative to the associated error showed adequate precision [34]. The ratio of the model was 40.795, indicating that the model was suitable for the design area [30]. In line with Table 4, the three variables which gave significant individual effects on oil removal were PASC dose (X_1), FP-1 dosage (X_2), and pH (X_3). The analysis also listed that they still had a significant quadratic effect (X_1^2, X_2^2, and X_3^2).

The diagnostic plots of predicted vs. actual values are illustrated in Fig. 1. The observed points of the actual values are distributed near to the predicted line, demonstrating there is a satisfying agreement between the suitable model and experimental data [16]. The response surfaces of the oil removal rate are shown in Fig. 2 with two different factors appeared an obvious peak in the boundary of response surfaces, demonstrating that the fitted conditions were within the design range [35].

Table 4
ANOVA for oil removal

Source	Sum of squares	DF	Mean square	*F*-value	*p*-value
Model	1,185.43	9	131.71	140.21	<0.0001
X_1	54.08	1	54.08	454.62	<0.0001
X_2	12.00	1	12.00	265.22	0.0020
X_3	48.02	1	48.02	319.51	<0.0001
X_1X_2	0.30	1	0.30	14.09	0.4728
X_1X_3	0.022	1	0.022	46.14	0.8420
X_2X_3	0.30	1	0.30	19.34	0.4728
X_1^2	304.39	1	304.39	180.66	<0.0001
X_2^2	297.27	1	397.27	174.59	<0.0001
X_3^2	356.57	1	356.57	207.93	<0.0001
Residual	3.68	7	0.53		
Lack of fit	2.71	3	0.90	3.73	0.1179
Pure error	0.97	4	0.24		
Total	1,189.11	16			

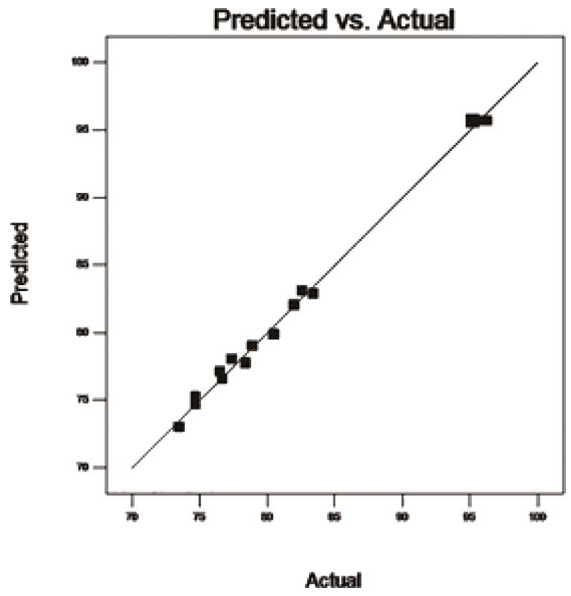

Fig. 1. Relationship between the predicted and measured oil removal efficiency.

There were interactive effects on oil removal between PASC dosage and FP-1 dosage, PASC dosage, and pH, as well as FP-1 dosage and pH. What is noteworthy in Fig. 2 is that oil removal gradually increased with an increase in PASC, FP-1, and pH and then declined, which is in view of the fact that when flocculants dosage was excess, the flocs were destroyed which indirectly led the suspended solid to disperse in the sample again [15,24]. On the other hand, charge neutralization was the main mechanism of aluminum ions in the coagulation process in the pH range of 4.0–5.5. When pH is 6.0–8.0, aluminum ions tend to the formation of amorphous $Al(OH)_3$, which removes pollutants by adsorption on the precipitation of $Al(OH)_3$ through the sweep-flocs mechanism [35,53]. The optimal pH 5.1 without the process of adjusting the pH was convenient and beneficial to the improvement of cationic charge density.

During coagulation, since FP-1 had higher density of positive charges, it may neutralize the oil's negative charges. The combined use of varied cationic organic flocculants (FP-1) may adsorb the colloids at the synergistic effect. Besides, positive charge's mutual superposition of FP-1 could improve the ability of charge neutrality.

Compared with poly aluminum chloride, the adding silicon may increase polymeric species and extensibility, which enabled the formation of a coagulant bridge and facilitated the formation of settleable flocs in coagulation–flocculation. PASC with cationic organic flocculants promoted the system to bridge between dispersed oil droplets and suspended solids, aggregate colloid, and contribute the particles to form sufficient size. The flocs formed by PASC were larger and denser, in view of which, the settlement of the suspended solid efficiently.

To achieve maximum desirability of oil removal and considering economic constraints, for each coagulant separately, the pH was set at original and the dose was kept at a minimum value [34]. In line with the results of the BBD, the optimum dose for maximum oil removal (96.09) for PASC, FP-1 and pH was 1.45, 2.2 g L^{-1}, and 5.14, respectively. To verify the reliability of the desired model, the AWE was treated at these optimal conditions, which indicates that the measured oil removal efficiency was 97.1% that was close to the predicted value, demonstrating that the RSM can optimize the reasonable coagulation–flocculation conditions for the AWE treatment.

3.2. Analysis of COD removal

The obtained COD removal rates under different experimental conditions are shown in Table 3. The following Eq. (5) of the model in terms of experimental data was obtained:

$$Y_1 = 89.68 - 2.71X_1 + 1.34X_2 + 2.65X_3 - 0.48X_1X_2 + 0.35X_1X_3 + 0.60X_2X_3 - 7.90X_1^2 - 8.05X_2^2 - 8.88X_3^2 \quad (5)$$

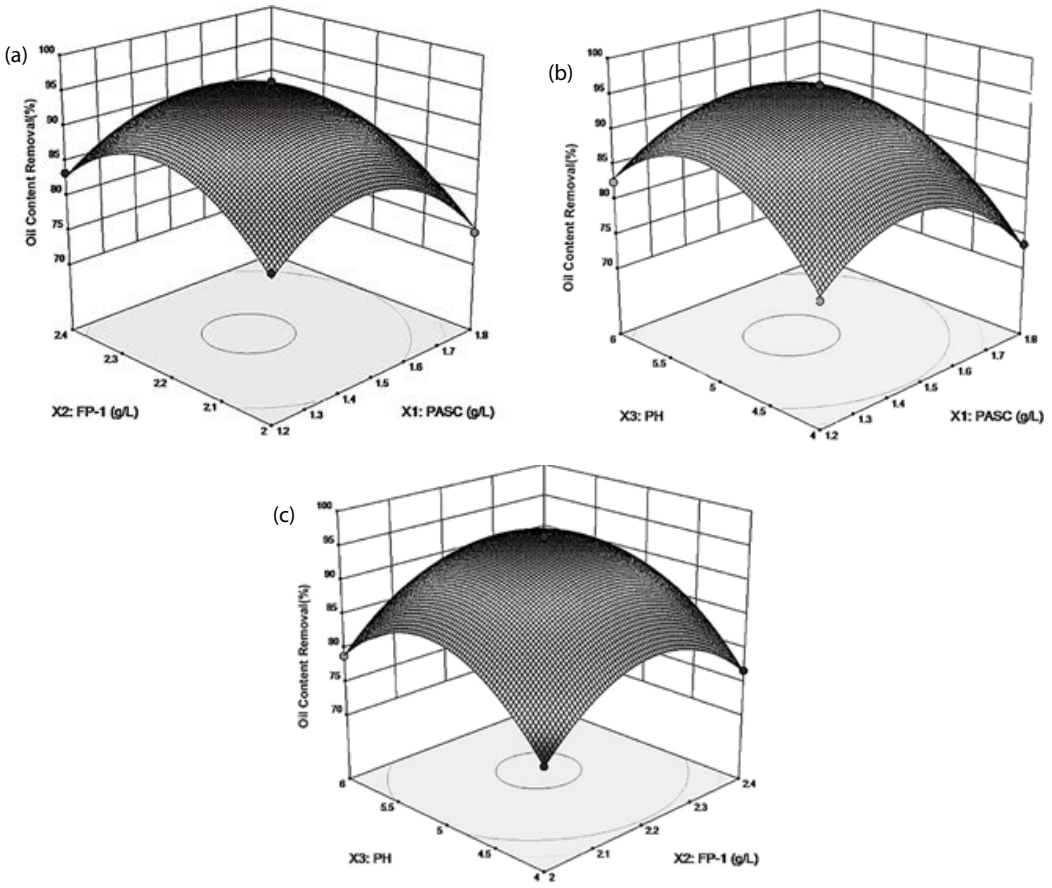

Fig. 2. (a) Surface graphs of oil removal showing the effect of variables PASC dosage–FP-1 dosage (pH: 5), (b) surface graphs of oil removal showing the effect of variables PASC dosage-pH (FP-1 dosage is 2.2 g L^{-1}), and (c) surface graphs of oil removal showing the effect of variables FP-1 dosage-pH (PASC dosage is 1.5 g L^{-1}).

In the light of ANOVA shown in Table 5, the regression model was statistically significant to explain the relationship between the COD removal efficiency and three variables, with no significant lack of fit (0.1015), a high regression coefficient (R^2 = 0.9957) and adjusted R^2 of 0.9901 [51]. The F-value of the model (F = 178.50) with an extremely small p-value (<0.0001) was used to justify the model was significant for fitting the experimental results well [35,50]. The predicted R^2 of 0.9458 was in reasonable agreement with the adjusted R^2. The ratio of 35.413 in the case of COD removal was an adequate signal. X_1, X_2, X_3, X_1^2, X_2^2, and X_3^2 were quite significant factors ($p < 0.01$). PASC dose, FP-1 dose, and pH were the considerable factors for COD removal rate. The p-values of X_1X_2, X_1X_3, and X_2X_3 were obviously smaller than them in oil removal, indicating that the interactive effect of these factors has a bigger impact on COD removal than on oil removal. The data in Fig. 3 illustrated the diagnostic plots of predicted responses vs. actual experimental data.

In line with the surface response curves (Fig. 4), as the dosage and pH increase the COD removal first increased and then decreased.

It is evident that the response surfaces of the oil and COD removal manifested in Figs. 2 and 4 had the similar tendency. The predicted responses vs. actual experimental data plots of oil and COD removal in Figs. 1 and 4 implied that the experimental value distribution of oil removal rate was similar to the COD removal rate. The rolling oil of AWE containing fats and fatty esters will be oxidized to increase the COD. Furthermore, the COD removal achieved the highest level as the oil removal approached to the maximum, demonstrating that oil was the main source which led to a high value of COD in the AWE. Consequently, oil removal was the most significant factor to COD removal of the AWE.

The obtained results demonstrated that the maximum removal of COD (90.17%) was achieved in dosage of PASC 1.45 and 2.22 g L^{-1} FP-1 and pH 5.14. The practical COD removal efficiency was obtained as 91.5% under the compromised condition, demonstrating that the confirmation experiment was a satisfying agreement with the model prediction. It is thoughtful that the specious efficiencies can be achieved at original pH of AWE based on our experiment results. Consequently, there is a balance in the industrial application between the cost for adjusting pH and the efficiency of the treatment, which revealed that the AWE could be treated without adjusting pH when the oil and COD removal efficiency were fulfilled and the cost for pH adjustment is a big concern [35].

Table 5
ANOVA for COD removal

Source	Sum of squares	DF	Mean square	*F*-value	*p*-value
Model	1,101.69	9	122.41	178.50	<0.0001
X_1	58.86	1	58.86	85.83	<0.0001
X_2	14.31	1	14.31	20.87	0.0026
X_3	56.18	1	56.18	81.92	<0.0001
X_1X_2	0.90	1	0.90	1.32	0.2890
X_1X_3	0.49	1	0.49	0.71	0.4259
X_2X_3	1.44	1	1.44	2.10	0.1906
X_1^2	262.95	1	262.95	383.42	<0.0001
X_2^2	273.02	1	273.02	398.12	<0.0001
X_3^2	331.83	1	331.83	483.87	<0.0001
Residual	4.80	7	0.69		
Lack of fit	3.63	3	1.21	4.15	0.1015
Pure error	1.17	4	0.29		
Total	1,106.49	16			

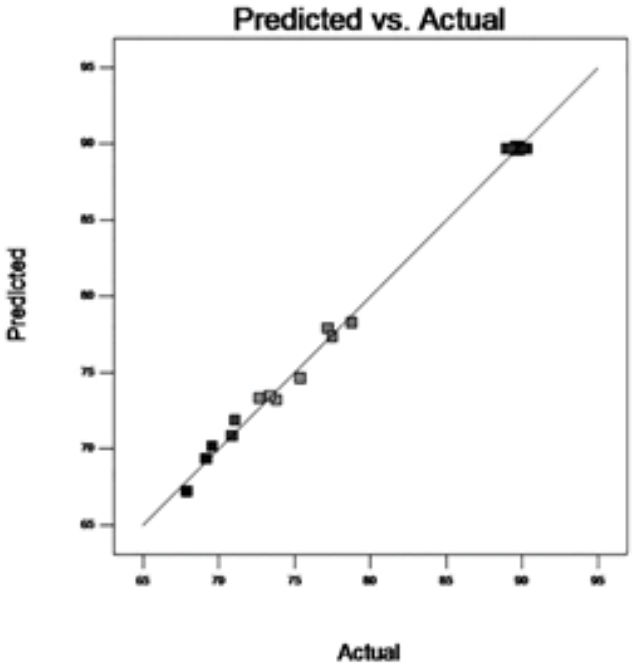

Fig. 3. Relationship between the predicted and measured COD removal efficiency.

3.3. Effect of settling time

Settling time had a direct influence on the effect of flocculation. A series of tests were measured to investigate the flocculation efficiencies of composite flocculants under various settling time (1, 3, 5, 10, 20, 30, 40, 50, 60, 70, and 80 min). The removal rates of COD and oil reached 91.5% and 97.1%, respectively, with the value of PASC/FP-1/pH (1.45 g L^{-1}/2.2 g L^{-1}/5.1) at 323 K at the settling time of 50 min. What was noteworthy in Figs. 5 and 6 was that the oil and COD removal rates would be extremely low if the settling time was excessively short, which was in view of the fact that some of the small flocs and suspended organic matter would not reach the top of the beakers. The oil droplets attached to the flocs formed by PASC and FP-1 needed a long time to settle. The removal rate of COD and oil would increase with the increasing of settling time, yet it would stay constant when the settling time reached the optimal one (50 min).

3.4. Effect of settling temperature

A series of tests were conducted for AWE at settling temperatures between 303 and 343 K with the mass concentration of PASC/FP-1/pH (1.45 g L^{-1}/2.2 g L^{-1}/5.1) and a settling time of 50 min. With increased temperature, the treatment efficiency demonstrated in Figs. 7 and 8 increased obviously and then became nearly constant. The optimal temperature is 328 K, where oil and COD removal efficiency was 97.1% and 91.5%, which could be concluded that heating-up not only strengthened Brownian motion of the particles in O/W emulsion to make them collided and coagulated effectively, but fell the internal viscosity of emulsion body greatly to weaken the stability of O/W emulsion [54]. As the temperature was increased further, the oil and COD content changed slowly. When the temperature reached a certain value, there was a balance of flocculation efficiency between organic and inorganic flocculants, which made oil and COD removal efficiency rates did not increase, which was accounted for by that the polymer FP-1 curled fast from the extended state, making the function of sweeping and bridging weaker with the increasing of temperature. Compared with organic flocculants, the molecular shape of inorganic flocculants which have the lower molecular weight cannot change so much with the increasing of temperature, which improved the flocculation efficiency [55].

3.5. Coagulation–flocculation mechanism

3.5.1. Optical microscope

To have a better understanding of the coagulation–flocculation process, the micro-morphologies of the AWE

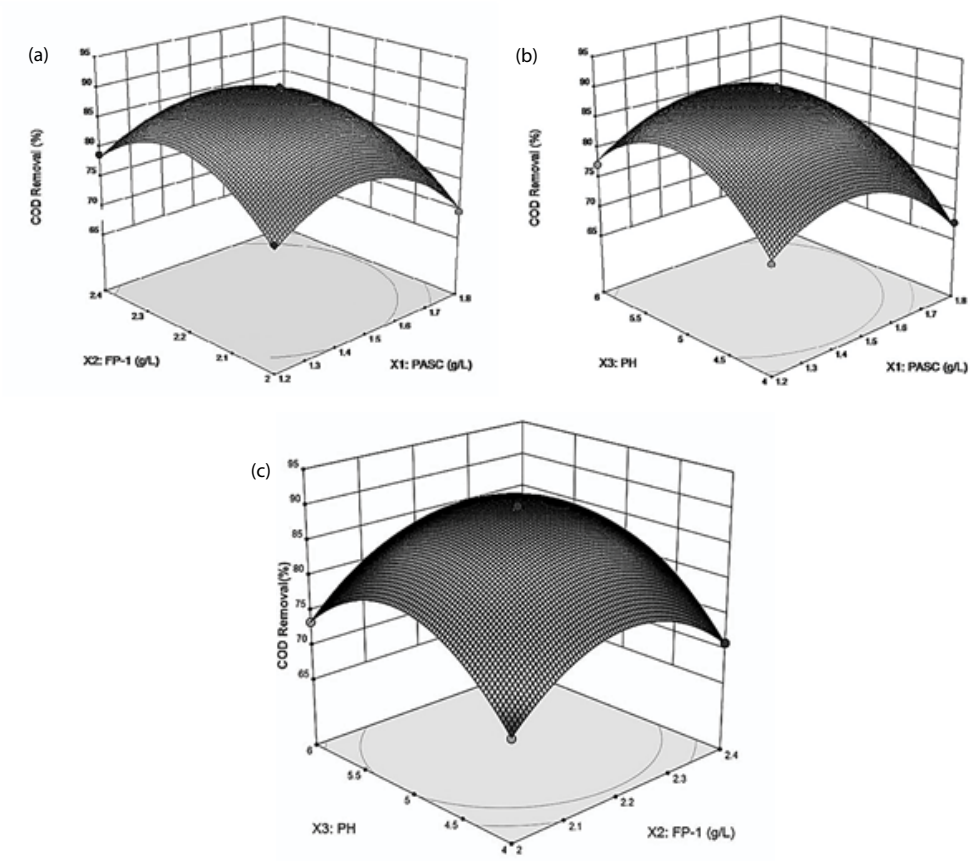

Fig. 4. (a) Surface graphs of COD removal showing the effect of variables PASC dosage–FP-1 dosage (pH:5), (b) surface graphs of COD removal showing the effect of variables PASC dosage-pH (FP-1 dosage is 2.2 g L^{-1}), and (c) surface graphs of COD removal showing the effect of variables FP-1 dosage-pH (PASC dosage is 1.5 g L^{-1}).

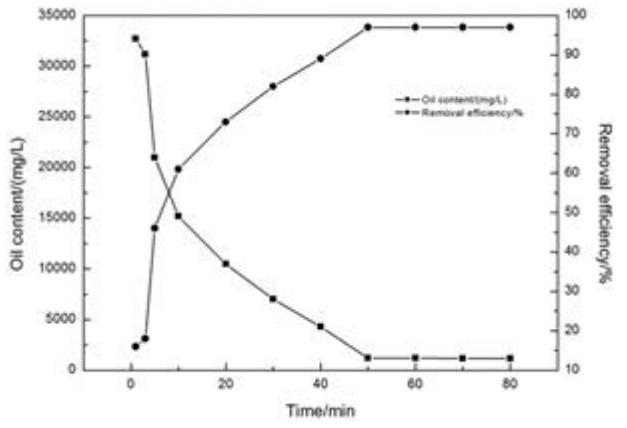

Fig. 5. Effect of settling time on oil content in demulsified water phase.

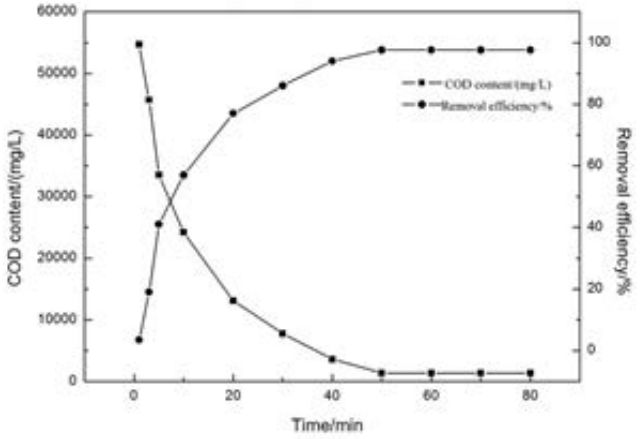

Fig. 6. Effect of settling time on COD content in demulsified water phase.

before and after coagulation–flocculation were observed by dint of utilizing an optical microscope. The microstructures of oil droplets before coagulation–flocculation in Fig. 9(a) appeared a regular and stable small circle. The microstructure of oil droplets after coagulation–flocculation in Fig. 9(b) was no longer a small round and appeared irregular shape. Figs. 9(c) and (d) show the enlarged irregularly shaped part of Fig. 9(b). It was observed that the oil droplets were homogeneously distributed in the water phase (Fig. 9(a)). Small amount of water was permeated into the destroyed oil phase after coagulation–flocculation (Fig. 9(b)).

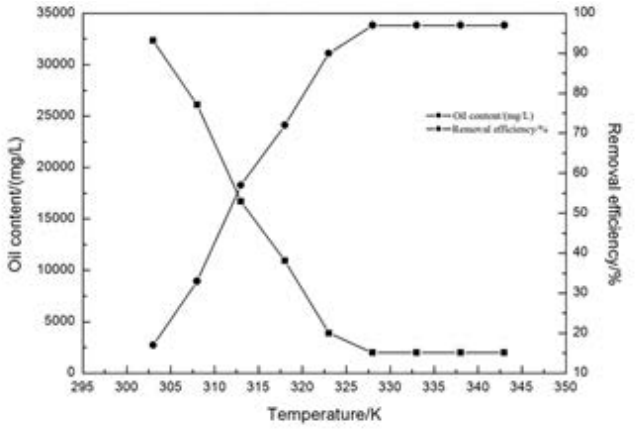

Fig. 7. Effect of temperature on oil content in demulsified water phase.

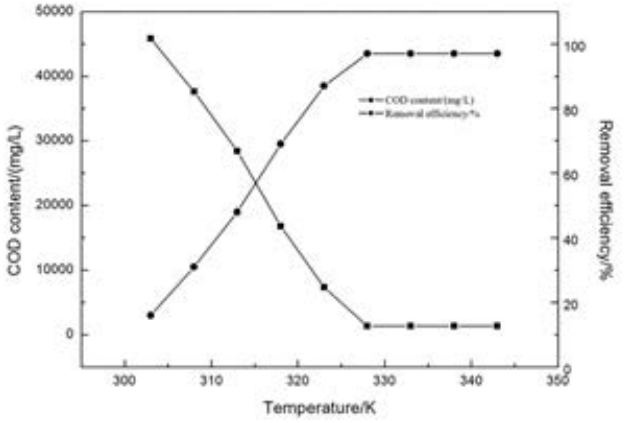

Fig. 8. Effect of temperature on COD content in demulsified water phase.

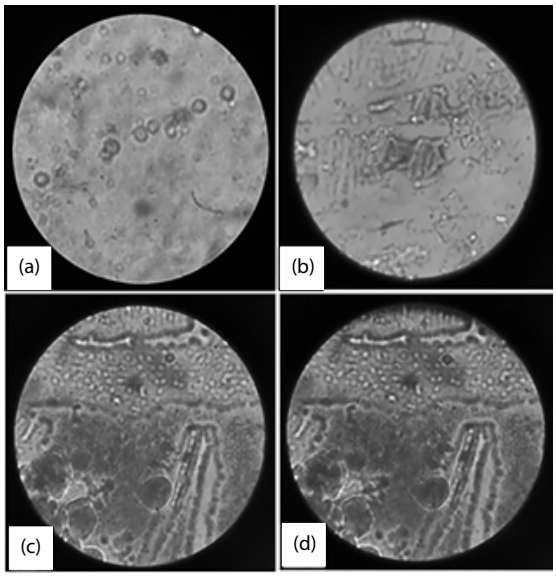

Fig. 9. Micrographs of (a) droplet microstructure of the emulsion before demulsification, (b) droplet microstructure of the emulsion after demulsification, (c), (d) the part of micrograph (b) enlarged.

These photos demonstrated that the added demulsifiers might neutralize negative charges on the surface of small oil droplets, which reduced the repulsive forces between the small oil droplets and promoted the formation of large, irregular oil droplets. In addition, these flocculants may remove the surfactants in the emulsion and destroy the structure of oil droplets in some way, making the solid surface of oil film soften.

3.5.2. FTIR spectra analysis

The FTIR spectra of FP-1 were studied to characterize the functional groups. The FTIR spectra of FP-1 exhibited peak locations, such as bands in the regions of 3,425, 1,660, and 1,600 cm^{-1},which depicted the amino group, the C=O stretching vibration of acylamino group, and the N–H bending vibration of acylamino group, respectively (Fig. 10).

Analyzing the spectrum, there were two absorption peaks of water at 2,116 and 1,639 cm^{-1} indicating that the FP-1 was hard to get absolute dry samples. There was a group of adsorption peaks at 2,700~3,000 cm^{-1}, which was in view of the stretching vibration peaks of methyl ($–CH_3$) and methylene ($–CH_2$). The strong absorption band at 3,413 cm^{-1} could be assigned to the O–H or N–H vibration peak in the structure. The absorption peak at 1,112 cm^{-1}which was resulted from the bonding C–N that was observed. The absorption peak at 980 cm^{-1} supported the formation of quaternary ammonium salt.

Figs. 11(a) and (b) illustrated that the FTIR spectra of samples of the oil from AWE and the oil from treated AWE. These similar peak locations at 2,900, 2,850, 1,730, and 1,720 cm^{-1} were observed in both the samples. The absorption peaks at 1,610 and 997 cm^{-1} belonging to the acylamino group and FP-1 are clearly seen, indicating that the FP-1 worked and remained in the oil phase. Comparing with Figs. 11(a) and (b), it was apparent that the two peaks of ester slightly change, indicating that FP-1 had an effect on the ester group. During coagulation–flocculation, the addition of positively charged quaternary ammonium from FP-1 may combine with the negative charges and stay in the oil phase.

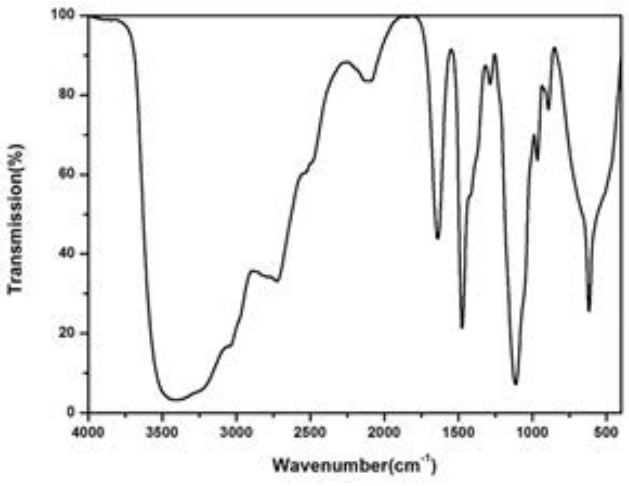

Fig. 10. FTIR spectra of FP-1.

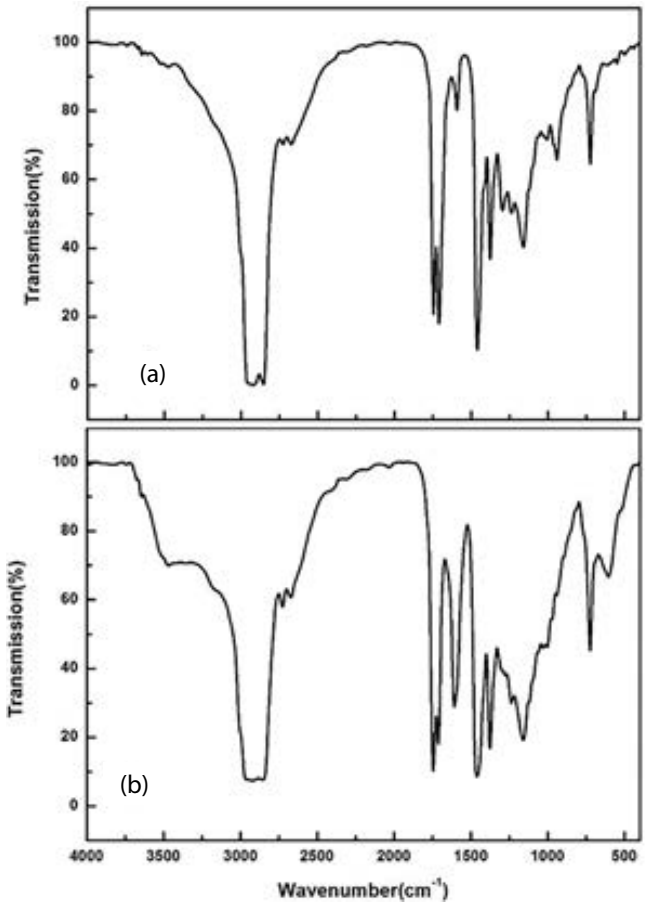

Fig. 11. FTIR spectrum of (a) the oil from AWE and (b) the oil from treated AWE.

3.5.3. SEM micrograph and EDS analyses

Fig. 12 is quite revealing to indicate the SEM micrographs. Micrographs (Figs. 12(b) and (c)) demonstrated the enlarged parts of micrograph (12(a)). It is apparent from Fig. 12(a) that the hydrolyzing aggregation produced by PASC and FP-1 were adhered to the particle surface of AWE. The particles were congregated to form the big flocs and massed further. It can be inferred from micrographs that the flocs generated after treatment of the AWE were porous and had more surface area. A strong honeycombed structure was observed in these micrographs, with suspended particulate matter entrapped in it, indicating sweeping flocculation of the PASC in the AWE [30]. The uneven surface of flocs was seen due to the occupation of flocculants on the oil molecules surface, indicating that flocculants could be employed effectively for treating AWE.

The data in Fig. 13 indicate the chemical composition of the flocs. The corresponding elemental mapping images clearly indicated that the upper flocs of the emulsion had the higher proportion of carbon and aluminum. The silicon (Si^{4+}) was stayed in the flocs, which indicated that the silicon was successfully introduced in PASC and played a significant role in demulsification.

3.5.4. Zeta potential

To obtain further insight into the coagulation–flocculation process, the zeta potentials of the liquid droplets were measured before and after adding 1.45 g L^{-1} PASC, 2.2 g L^{-1} FP-1 to AWE at 55°C, pH 5.1. As a result, it could be found that the zeta potential of the original emulsion was negative and the value was –40.0 mV (Fig. 14), indicating that the emulsion was stabilized by the electrostatic repulsion between the dispersed electronegative oil droplets.

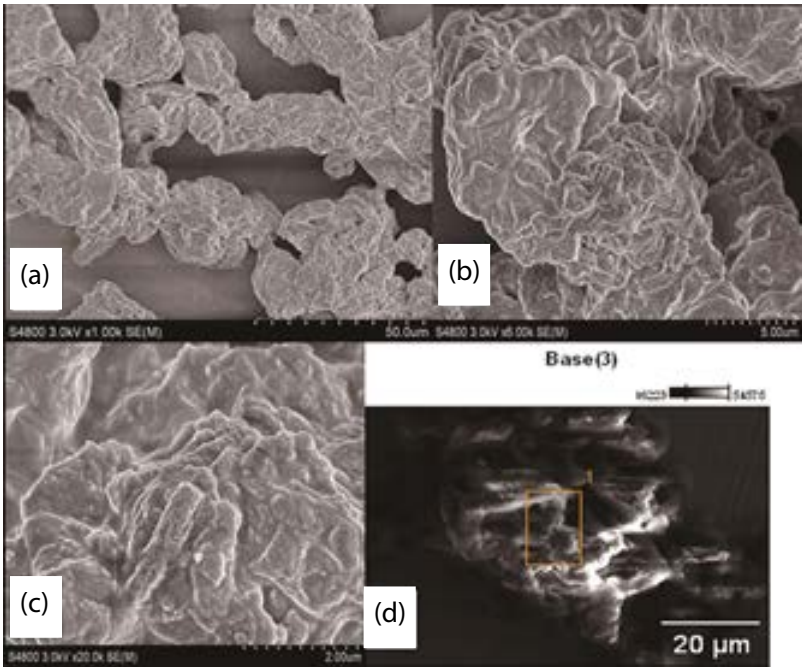

Fig. 12. SEM images of (a), (b), (c), (d) the upper floc of the emulsion after demulsification at different resolutions.

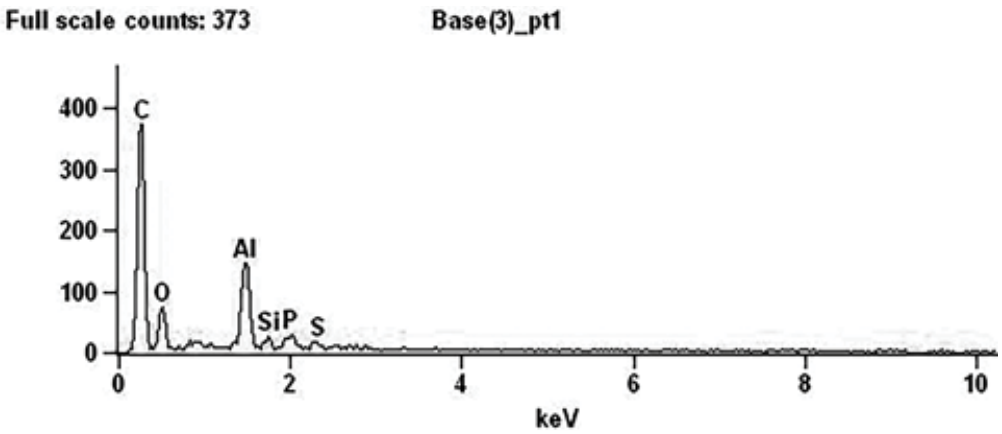

Fig. 13. Energy spectrum diagram of the flocs of the emulsion after demulsification.

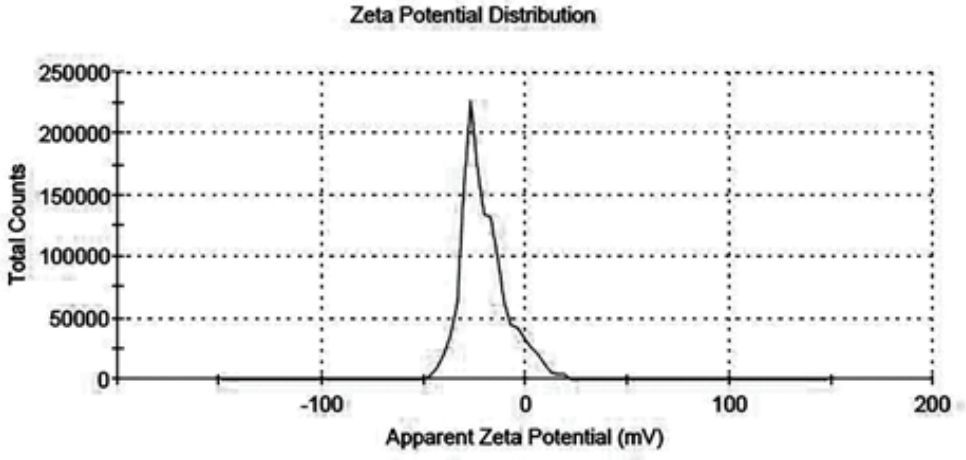

Fig. 14. Zeta potential of the original emulsion.

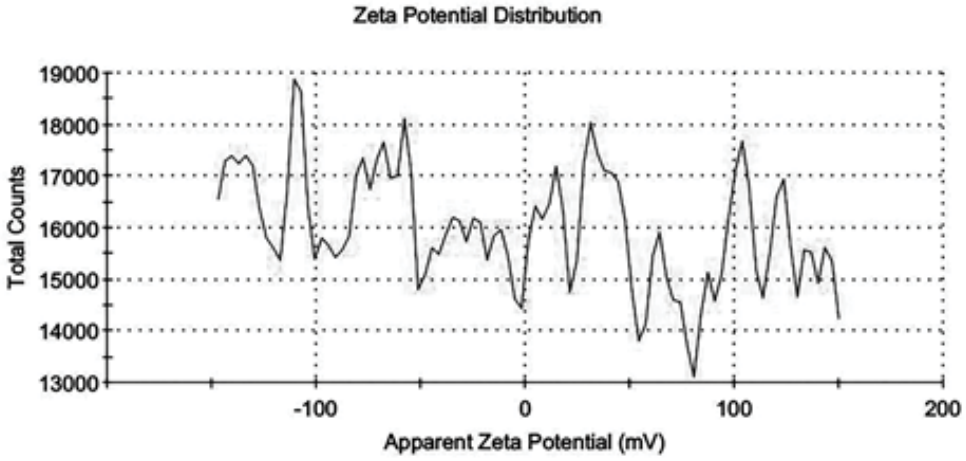

Fig. 15. Zeta potential of the original emulsion tends to demulsification.

When increasing the mass concentration of PASC and FP-1, zeta potential was close to 0 mV, which indicated that these charges on the particle surface were almost completely neutralized, even turned to be positive. Simultaneously, the distribution of zeta potentials appears uneven multi-peaks (Fig. 15). The occurrence of multiple peaks may be in view of the increasing collisions and movements of charges in the emulsion, resulting in agglomerating of particles, making the movement resistance and scattering ability stronger. In any event, the zeta potential after breaking up changed to

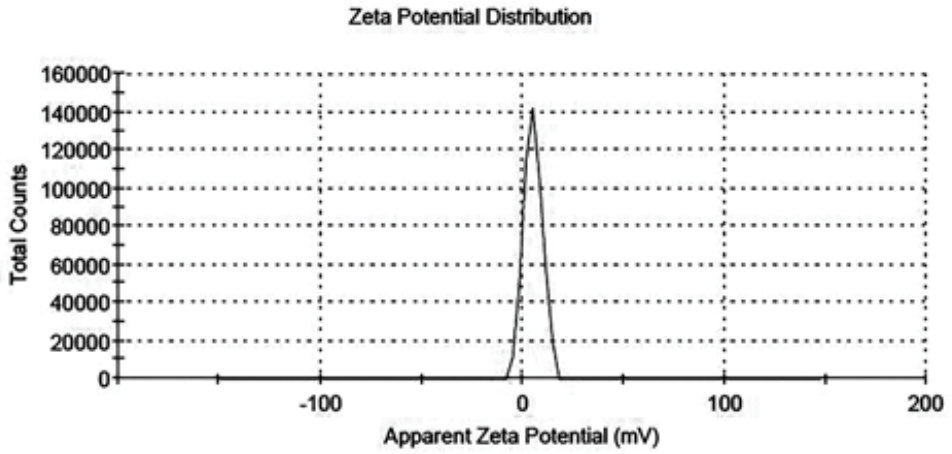

Fig. 16. Zeta potential of the water phase after demulsification.

5.38 mV. The zeta potential map showed a single peak again, indicating that the system has reached another new steady state (Fig. 16).

4. Conclusions

The coagulation–flocculation process with PASC and FP-1 as the demulsifiers was employed for AWE. The RSM and BBD were used with the aim of hitting the goal of maximizing the removal of oil and COD to optimize reaction conditions and determine the influences and interactions of three factors (PASC dose, FP-1 dose, and pH). The results revealed that the desired COD and oil removal efficiencies could reach 91.5% and 97.1% by dint of employing 1.45 g L^{-1} PASC, 2.22 g L^{-1} FP-1 at pH 5.1 and 328 K. The results indicated that the combination of PASC and epichlorohydrin amine cationic polymer (FP-1) may have better demulsification at the synergistic effect than a single inorganic flocculant in neutralizing charge and agglomerating the destabilized colloidal particles. FTIR, zeta potentials, and SEM-EDS were utilized to study the mechanism of electric neutralization, adsorption, and sweep in the coagulation–flocculation process of AWE. The employing of PASC and cationic organic flocculant (FP-1) without adjusting pH has practical significance for the treatment of AWE or O/W emulsion.

Acknowledgments

The authors are grateful to the financial support of Major National Science and Technology Projects (2017ZX07402003), the Natural Science Foundation of Tianjin City (16JCQNJC03200) and the National Science and Technology Major Project 40 for Subject 5 during the Thirteenth Five-year Plan Period (2016ZX05040-005).

References

[1] L. Zhang, Y. Wang, S. Ni, G. Chen, K. Li, Y. Du, M. Song, The evolution of second-phase particles in 6111 aluminum alloy processed by hot and cold rolling, J. Mater. Eng. Perform., 27 (2018) 1130–1137.
[2] W.S. Miller, L. Zhuang, J. Bottema, A.J. Wittebrood, P. De Smet, A. Haszler, A. Vieregge, Recent development in aluminium alloys for the automotive industry, Mater. Sci. Eng. A, 280 (2000) 37–49.
[3] A.R. Riahi, O.A. Gali, K.R. Januszkiewicz, D. Pattemore, Experimental study of the disturbed layer generation during hot rolling contact of aluminum with steel, Tribol. Int., 54 (2012) 42–50.
[4] Y. Okamoto, Oil Compositions for Hot Rolling Aluminum and Aluminum Alloys, U.S. Patent 5,583,100[P].1996-12-10.
[5] F.E. Lockwood, K. Bridger, M.E. Tadros, Interactions between rolling oil emulsions and aluminum alloy surfaces, ASLE Trans., 27 (1984) 203–206.
[6] M.S. Chun, J.G. Lenard, Hot rolling of an aluminum alloy using oil/water emulsions, J. Mater. Process. Technol., 72 (1997) 283–292.
[7] A. Shirizly, J.G. Lenard, J. Sauer, K. Januszkiewicz, Lubricant capture during hot rolling of an aluminum alloy, Tribol. Trans., 45 (2002) 205–210.
[8] A. Johnsson1, M. Ekman, A. Janols, Developing environmentally friendly rolling lubricants, J. Eng. Tribol., 225 (2011) 932–939.
[9] D. Han, Aluminum alloy slab band hot rolling emulsion electrolysis breaking device has waste liquid tank that includes vent at bottom of stirring unit and steam heating unit, and waste electrolytic device that includes anode and cathode plates: CN. Patent 202,682,851-U [P].2013-1-23.
[10] Y. Liu, C.C. Lv, J. Ding, P. Qian, X.M. Zhang, Y. Yu, S.F. Ye, Y.F. Chen, The use of the organic–inorganic hybrid polymer $Al(OH)_3$–polyacrylamide to flocculate particles in the cyanide tailing suspensions, Miner. Eng., 89 (2016) 108–117.
[11] J.Y. Yang, L. Yan, S.P. Li, X.R. Xu, Treatment of aging oily wastewater by demulsification/flocculation, J. Environ. Sci. Health. Part A Toxic/Hazard. Subst. Environ. Eng., 51 (2016) 1–7.
[12] D.F. Zeng, D. Hu, J. Cheng, Preparation and study of a composite flocculant for papermaking wastewater treatment, J. Environ. Prot., 2 (2011) 1370–1374.
[13] Z.C. Zhang, The flocculation mechanism and treatment of oily wastewater by flocculation, Water Sci. Technol., 76 (2017) 2630–2637.
[14] K.E. Lee, T.T. Teng, N. Morad, B.T. Poh, Y.F. Hong, Flocculation of kaolin in water using novel calcium chloride-polyacrylamide ($CaCl_2$-PAM) hybrid polymer, Sep. Purif. Technol., 75 (2010) 346–351.
[15] Y.B. Zeng, C.Z. Yang, J.D. Zhang, W.H. Pu, Feasibility investigation of oily wastewater treatment by combination of zinc and PAM in coagulation/flocculation, J. Hazard. Mater., 147 (2007) 991–996.
[16] Y. Yang, Y. Li, Y.M. Zhang, D.W. Liang, Applying hybrid coagulants and polyacrylamide flocculants in the treatment of high-phosphorus hematite flotation wastewater (HHFW): optimization through response surface methodology, Sep. Purif. Technol., 76 (2010) 72–78.

[17] P.A. Moussas, A.I. Zouboulis, A new inorganic–organic composite coagulant, consisting of polyferric sulphate (PFS) and polyacrylamide (PAA), Water Res., 43 (2009) 3511–3524.
[18] H.S. Kim, D.J. Joo, J. Lee, Flocculating properties of polycondensate of 1-Butyl Amine and Epichlorohydrin, Environ. Technol., 20 (1998) 117–120.
[19] Q. Li, Q.Y. Yue, H.J. Sun, Y. Su, B.Y. Gao, A comparative study on the properties, mechanisms and process designs for the adsorption of non-ionic or anionic dyes onto cationic-polymer/bentonite, J. Environ. Manage., 91 (2010) 1601–1611.
[20] Q. Li, Q.Y. Yue, Y. Su, B.Y. Gao, Equilibrium and a two-stage batch adsorber design for reactive or disperse dye removal to minimize adsorbent amount, Bioresour. Technol., 102 (2011) 5290–5296.
[21] G.J. Churchman, Formation of complexes between bentonite and different cationic polyelectrolytes and their use as sorbents for non-ionic and anionic pollutants, Appl. Clay Sci., 21 (2002) 177–189.
[22] Y.P. Jin, Y.H. Wu, J.l. Cao, Y.Y. Wu, Optimizing decolorization of Methylene Blue and Methyl Orange dye by pulsed discharged plasma in water using response surface methodology, J. Taiwan Inst. Chem. Eng., 45 (2014) 589–595.
[23] B.Y. Tak, B.S. Tak, Y.J. Kim, Y.J. Park, Y.H. Yoon, G.H. Min, Optimization of color and COD removal from livestock wastewater by electrocoagulation process: application of Box–Behnken design (BBD), J. Ind. Eng. Chem., 28 (2015) 307–315.
[24] Y.F. Wang, K.F. Chen, L.H. Mo, J. Li, J. Xu, Optimization of coagulation–flocculation process for papermaking-reconstituted tobacco slice wastewater treatment using response surface methodology, J. Ind. Eng. Chem., 20 (2014) 391–396.
[25] S.S. Kumar, N.R. Bishnoil, Coagulation of landfill leachate by $FeCl_3$: process optimization using Box–Behnken design (RSM), Appl. Water Sci., 7 (2017) 1943–1953.
[26] C. Desjardins, B. Koudjonou, R. Desjardins, Laboratory study of ballasted flocculation, Water Res., 36 (2002) 744–754.
[27] A. Gürses, M. Yalçin, C. Dogar, Removal of *Remazol Red Rb* by using Al (III) as coagulant-flocculant: effect of some variables on settling velocity, Water Air Soil Pollut., 146 (2003) 297–318.
[28] S.M.R. Shaikh, M.S. Nasser, I.A. Hussein, A. Benamor, Investigation of the effect of polyelectrolyte structure and type on the electrokinetics and flocculation behavior of bentonite dispersions, Chem. Eng. J., 311 (2017) 265–276.
[29] Z.Z. Liu, H. Wei, A.M. Li, H. Yang, Evaluation of structural effects on the flocculation performance of a co-graft starch-based flocculant, Water Res., 118 (2017) 160–166.
[30] Q.B. He, C. Deng, Y. Xu, D.N. Shen, B. Dong, X.H. Dai, Optimization of and mechanism for the coagulation–flocculation of oil-field wastewater from polymer flooding, Desal. Wat. Treat., 57 (2016) 1–10.
[31] C.Z. Hu, H.J. Liu, J.H. Qu, D.S. Wang, J. Ru, Coagulation behavior of aluminum salts in eutrophic water: significance of Al_{13} species and pH control, Environ. Sci. Technol., 40 (2006) 325–331.
[32] S.M. Miller, E.J. Fugate, V.O. Craver, J.A. Smith, J.B. Zimmerman, Toward understanding the efficacy and mechanism of *Opuntia* spp. as a natural coagulant for potential application in water treatment, Environ. Sci. Technol., 42 (2008) 4274–4279.
[33] K.J. Howe, A. Marwah, K.P. Chiu, S.S. Adham, Effect of coagulation on the size of MF and UF membrane foulants, Environ. Sci. Technol., 40 (2006) 7908–7913.
[34] S. Mukherjee, A. Pariatamby, J.N. Sahu, B.S. Gupta, Clarification of rubber mill wastewater by a plant based biopolymer-comparison with common inorganic coagulants, J. Chem. Technol. Biotechnol., 88 (2013) 1864–1873.
[35] J.P. Wang, Y.Z. Chen, Y. Wang, S.J. Yuan, H.Q. Yu, Optimization of the coagulation-flocculation process for pulp mill wastewater treatment using a combination of uniform design and response surface methodology, Water Res., 45 (2011) 5633–5640.
[36] N. Birjandi, H. Younesi, N. Bahramifar, S. Ghafari, A.A. Zinatizadeh, S. Sethupathi, Optimization of coagulation-flocculation treatment on paper-recycling wastewater: application of response surface methodology, J. Environ. Sci. Health. Part A Toxic/Hazard. Subst. Environ. Eng., 48 (2013) 1573–1582.
[37] R. Lessoued, F. Souahi, L.C. Pelaez, Modelization and statistical optimization of coagulation–flocculation treatment of an old leachate, Water Environ. Res., 89 (2017) 2136–2141.
[38] N.M. Daud, S.R.S. Abdullah, H.A. Hasan, Response surface methodological analysis for the optimization of acid-catalyzed transesterification biodiesel wastewater pre-treatment using coagulation–flocculation process, Process Saf. Environ. Prot., 113 (2018) 184–192.
[39] W. Setyaningsih, I.E. Saputro, C.A. Carrera, M. Palma, C.G. Barroso, Multiresponse optimization of a UPLC method for the simultaneous determination of tryptophan and 15 tryptophan-derived compounds using a Box-Behnken design with a desirability function, Food Chem., 225 (2017) 1–9
[40] Y.J. Shen, Y. Wang, J. Shi, D.P. Tan, X.H. Jing, Q.H. Xu, Modeling and optimization of the electric flocculation of wastewater containing Cr^{6+} using response surface methodology, Sep. Sci. Technol., 52 (2017) 2684–2695.
[41] X.R. Xu, G.L. Liu, Y.M. Yang, J.S. Gao, Study on demulsification of the oil-in-water emulsion from column top of a delayed coking unit in refinery. II. synthesis and application, Petrol. Sci. Technol., 22 (2004) 247–261.
[42] R. Zolfaghari, A. Fakhru'L-Razi, L.C. Abdullah, S.S.E.H. Elnashaie, A. Pendashteh, Demulsification techniques of water-in-oil and oil-in-water emulsions in petroleum industry, Sep. Purif. Technol., 170 (2016) 377–407.
[43] J. Liu, H.J. Wang, X.C. Li, W.H. Jia, Y.P. Zhao, S.L. Ren, Recyclable magnetic graphene oxide for rapid and efficient demulsification of crude oil-in-water emulsion, Fuel, 189 (2017) 79–87.
[44] R. Martínez-Palou, J. Reyes, R. Cerón-Camacho, M. Ramírez-de-Santiago, D. Villanueva, A.A. Vallejo, J. Aburto, Study of the formation and breaking of extra-heavy-crude-oil-in-water emulsions—a proposed strategy for transporting extra heavy crude oils, Chem. Eng. Process., 98 (2015) 112–122.
[45] W.L. Kang, L.M. Guo, H.M. Fan, L.W. Meng, Y.H. Li, Flocculation, coalescence and migration of dispersed phase droplets and oil–water separation in heavy oil emulsion, J. Petrol. Sci. Eng., 81 (2012) 177–181.
[46] A.A. Umar, I.B.M. Saaid, A.A. Sulaimon, R.B.M. Pilus, A review of petroleum emulsions and recent progress on water-in-crude oil emulsions stabilized by natural surfactants and solids, J. Petrol. Sci. Eng., 165 (2018) 673–690.
[47] K.A. Lin, Y.C. Chen, S. Phattarapattamawong, Efficient demulsification of oil-in-water emulsions using a zeolitic imidazolate framework: adsorptive removal of oil droplets from water, J. Colloid Interface Sci., 478 (2016) 97–106.
[48] M. Moradi, F. Ghanbari, Application of response surface method for coagulation process in leachate treatment as pretreatment for Fenton process: biodegradability improvement, J. Water Process Eng., 4 (2014) 67–73.
[49] S. Chattoraj, N.K. Mondal, B. Das, P. Roy, B. Sadhukhan, Biosorption of carbaryl from aqueous solution onto *Pistia stratiotes* biomass, Appl. Water Sci., 4 (2014) 79–88.
[50] R. Sen, T. Swaminathan, Response surface modeling and optimization to elucidate and analyze the effects of inoculum age and size on surfactin production, Biochem. Eng. J., 21 (2004) 141–148.
[51] M.A. Rasool, T. Babak, C. Naz, A.R. Pendashteh, A.S. Mirroshandel, Use of a plant-based coagulant in coagulation–ozonation combined treatment of leachate from a waste dumping site, Ecol. Eng., 90 (2016) 431–437.
[52] A. Lee, N. Chaibakhsh, M.B.A. Rahman, M. Basri, B.A. Tejo, Optimized enzymatic synthesis of levulinate ester in solvent-free system, Ind. Crops Prod., 32 (2010) 246–251.
[53] Q. Chang, J.Y. Fu, Z.L. Li, Principles of Flocculation, Lanzhou University Press, Lanzhou, 1993.
[54] H.Z. Zhang, S.M. Fang, C.M. Ye, M.H. Wang, H.J. Cheng, H. Wen, X.L. Meng, Treatment of waste filature oil/water emulsion by combined demulsification and reverse osmosis, Sep. Purif. Technol., 63 (2008) 264–268.
[55] X.F. Zhao, L.X. Liu, Y.C. Wang, H.X. Dai, D. Wang, H. Cai, Influences of partially hydrolyzed polyacrylamide (HPAM) residue on the flocculation behavior of oily wastewater produced from polymer flooding, Sep. Purif. Technol., 62 (2008) 199–204.